Biochemistry

 Volume 42, Number 47 December 2, 2003

Articles

Penetratin and Related Cell-Penetrating Cationic Peptides Can Translocate Across Lipid Bilayers in the Presence of a Transbilayer Potential†

Donato Terrone, Stephane Leung Wai Sang, Liya Roudaia, and John R. Silvius*

Department of Biochemistry, McGill University, Montréal, Québec, Canada H3G 1Y6

Received July 22, 2003; Revised Manuscript Received September 16, 2003

ABSTRACT: Fluorescent-labeled derivatives of the *Antennapedia*-derived cell-penetating peptide penetratin, and of the simpler but similarly charged peptides R_6GC-NH_2 and K_6GC-NH_2, are shown to be able to translocate into large unilamellar lipid vesicles in the presence of a transbilayer potential (inside negative). Vesicles with diverse lipid compositions, and combining physiological proportions of neutral and anionic lipids, are able to support substantial potential-dependent uptake of all three cationic peptides. The efficiency of peptide uptake under these conditions is strongly modulated by the vesicle lipid composition, in a manner that suggests that more than one mechanism of peptide uptake may operate in different systems. Remarkably, peptide uptake is accompanied by only minor perturbations of the overall barrier function of the lipid bilayer, as assessed by assays of vesicle leakiness under the same conditions. Fluorescence microscopy of living CV-1 and HeLa cells incubated with the labeled peptides shows that the peptides accumulate in peripheral vesicular structures at early times of incubation, consistent with an initial endosomal localization as recently reported, but gradually accumulate in the cytoplasm and nucleus during more extended incubations (several hours). Our findings indicate that these relatively hydrophilic, polybasic cell-penetrating peptides can translocate through lipid bilayers by a potential- and composition-dependent pathway that causes only minimal perturbation to the overall integrity and barrier function of the bilayer.

Cell-penetrating cationic peptides have attracted much interest in the light of their capacity to mediate cellular uptake and intracellular activity of associated peptide sequences, proteins, and other bioactive molecules (*1*, *2*). Many membrane-associating toxic peptides exhibit a markedly amphipathic character and appear to translocate across membranes by pore formation (*3*−*5*). By contrast, cell-penetrating peptides such as the *Antennapedia* homeodomain-derived peptide penetratin, the amino acid 48−60 sequence of the HIV Tat protein, and even simple polyarginine-based sequences (*6*−*9*) are highly positively charged but exhibit at most a very limited amphiphilic character and do not appear to form classical pores in lipid bilayers.

Early fluorescence-microscopic observations suggesting that cationic cell-penetrating peptides very rapidly traverse the plasma membrane have been challenged by more recent studies which suggest that in live, unfixed cells, after relatively short incubations, internalized peptide molecules are predominantly localized to endocytic compartments (*10*−*14*). Nonetheless, constructs linking various bioactive sequences to cell-penetrating peptides have been shown to produce clear biological effects in cellular compartments outside the endosomal/lysosomal system when incubated

† This work was supported by Grant MOP-7776 from the Canadian Institutes of Health Research (CIHR) to J.R.S., by funding from the CIHR Strategic Training Initiative in Chemical Biology to S.L.W.S., and by McGill University Graduate Studies Fellowship awards to D.T. and L.R.

* To whom correspondence should be addressed. Phone: (514) 398-7267. Fax: (514) 398-7384. E-mail: john.silvius@mcgill.ca.

10.1021/bi035293y CCC: $25.00
Published on Web 11/11/2003

with intact mammalian cells for periods of hours (*15*−*18*), and an exogenously added *Antennapedia*-derived peptide has been shown by microscopy to reach the cell nucleus after incubation on a similar time scale with cultured neurons (*19*). These observations suggest that rapid internalization of such peptides to the endosomal compartment may be followed by slower translocation to the cytoplasm, and thereby to other intracellular compartments if the peptides bear appropriate targeting signals.

If the initial interactions of cationic cell-penetrating peptides with mammalian cells are becoming clearer, the mechanism by which these peptides subsequently translocate to the cytoplasm (and thence to other nonendocytic compartments) remains enigmatic. A lipid-based pathway for membrane translocation of cell-penetrating peptides has been suggested based on the lack of clear evidence for sequence-specific determinants of peptide uptake (*7*, *12*), on findings that suggest a strong correlation of uptake with lipid-binding affinity (*20*), and on observations that penetratin can promote formation of nonlamellar structures in lipid extracts from embryonic rat brain, although not in mixtures of synthetic phosphatidylcholine (PC)[1] and phosphatidylserine (PS) (*21*). To date, however, studies of the ability of basic cell-penetrating peptides to translocate across model lipid bilayers have given divergent results. Drin et al. (*13*, *20*) found that penetratin did not translocate significantly on a time scale of a few tens of minutes into small unilamellar vesicles composed of mixtures combining synthetic PC with PS or phosphatidylglycerol (PG), and similar findings have been reported for the cell-penetrating Tat peptide (*23*). By contrast, fluorescence-microscopic findings have been reported which suggest that penetratin may traverse the membranes of giant unilamellar vesicles prepared from soybean asolectin (*24*). It has also been suggested that at very high ratios of bilayer-bound penetratin to lipid, the peptide may directly destabilize the bilayer through electrostatically induced stresses (*25*). It is not clear to what extent these divergent model-system findings may reflect differences in the composition, size, or other features of the lipid vesicles examined in each study. As noted previously, it is also possible that transmembrane movement of cell-penetrating peptides in living cells is rather slower than initially hypothesized, and than some model-system studies reported to date have been designed to examine.

In this study, we have examined the ability of penetratin and of two simpler peptides of comparable charge (R_6GC-NH_2 and K_6GC-NH_2) to traverse lipid membranes with diverse compositions, on a broad range of time scales and in the presence or absence of a transbilayer potential gradient. In the absence of a transbilayer potential, such peptides show at best very slow rates of translocation into lipid vesicles of diverse compositions. However, in the presence of a transbilayer potential, these peptides can translocate at significant rates into lipid vesicles, in a manner that is strongly influenced by the vesicle composition. Strikingly, the uptake of these polybasic peptides into vesicles can proceed with minimal perturbation of overall vesicle integrity, suggesting that the mechanism of transbilayer uptake for these species may differ substantially from that employed by more classical pore-forming amphiphilic peptides.

MATERIALS AND METHODS

Materials. Phospho- and sphingolipids were obtained from Sigma (St. Louis, MO) or Avanti Polar Lipids (Alabaster, AL). Lipid stock solutions were prepared in CH_2Cl_2 or CH_2Cl_2/methanol, standardized by phosphate determination (*26*), and stored under argon at −20 °C. Soybean asolectin (Sigma, L-α-phosphatidylcholine type II-S) was freed of neutral lipids as described by Kagawa et al. (*27*). Stock solutions of polyunsaturated lipids were prepared containing butylated hydroxytoluene (1:250 mol/mol lipid) and used within four weeks of preparation. Diphytanoyl *N*-(7-nitrobenz-2-oxa-1,3-diazol-4-yl)- and diphytanoyl *N*-(lissamine rhodamine B sulfonyl)-phosphatidylethanolamine (NBD-PE and Rho-PE) were synthesized as described previously (*28*, *29*). Purities of lipid stocks were monitored by TLC. Fluorescent labeling reagents were obtained from Molecular Probes (Eugene, OR).

The penetratin peptide with a carboxy-terminal glycyl-cysteinamide extension (RQKIWFQNRRMKWKKCG-NH_2, >95% purity as assessed by HPLC) was purchased from American Peptide Company (Sunnyvale, CA). R_6GC-NH_2 and K_6GC-NH_2 were synthesized by solid-phase synthesis using Fmoc chemistry and purified by HPLC. Peptide masses were confirmed by mass spectrometry. Fluorescent derivatives of these peptides were prepared by reacting 1−2 μmol of peptide overnight and under argon (with exclusion of light) with a 4-fold molar excess of *N*,*N*′-dimethyl-*N*-(iodoacetyl)-*N*′-(NBD)ethylenediamine (IANBD amide) or monobromobimane or for 6 h under argon with a 2-fold excess of Texas Red-C_2-maleimide, in 0.4 mL of 1:1 DMF/50 mM aq MOPS, pH 7.0. The reaction mixture was dried, and the labeled peptide was three times precipitated from a minimum volume of 1:1 methanol/10 mM aq NaCl with 6 mL of cold acetone, then redissolved in 250 μL of 2% aq acetic acid and passed through a 2.5 mL column of Sephadex G-15 (packed and eluted in 50 mM ammonium acetate) to remove a small slower-eluting fluorescent band. The eluted peptide was finally lyophilized, redissolved in 250 μL of sterile water, and stored in aliquots at −70 °C. TLC of the labeled peptide preparations on silica gel 60 plates (in 50:20:15:10:6 v/v/v/v/v CH_2Cl_2/acetone/methanol/acetic acid/water) showed complete removal of unconjugated fluorescent material.

MyristoylGlyHis-edNBD (mGH-edNBD) was prepared by successively coupling mono-*N*-NBD-ethylenediamine (*30*) to *N*-Fmoc-(τ-trityl)-histidine, to Fmoc-glycine, and finally to myristic acid, using methods described previously (*31*). After the final coupling reaction, the probe was side chain-deprotected by incubation in 66:33:4:4:2 CH_2Cl_2/trifluoroacetic acid/dimethyl sulfide/water/triethylsilane (25 °C, 1 h) and finally purified by preparative TLC in 75:25:1 (v/v/v) CH_2Cl_2/methanol/acetic acid. MyristoylGlyArgLys(NBD)-OH (mGRK(NBD)-OH) was prepared by a similar strategy but initially incorporating the lysine residue in its ε-*tert*-

[1] Abbreviations: DMF, dimethylformamide; DO-, dioleoyl- (PC, etc.); ePC, egg yolk phosphatidylcholine; LUV, large unilamellar vesicles; MOPS, 3-(*N*-morpholino)propanesulfonic acid; NBD-, 7-nitrobenz-2-oxa-1,3-diazol-4-yl-; NBD-PE, 1,2-diphytanoyl *N*-NBD-phosphatidylethanolamine; PA, phosphatidic acid; PC, phosphatidylcholine; PE, phosphatidylethanolamine; PG, phosphatidylglycerol; PO-, 1-palmitoyl-2-oleoyl- (PC, etc.); PS, phosphatidylserine; Rho-PE, diphytanol *N*-(lissamine rhodamine B sulfonyl)-phosphatidylethanolamine; soy PI, phosphatidylinositol from soybean; tPE, PE prepared from egg PC by transphosphatidylation; TLC, thin-layer chromatography.

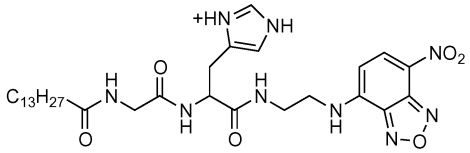

myristoylGlyHis-edNBD (mGH-edNBD)

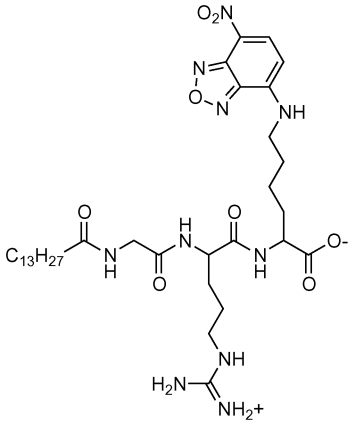

myristoylGlyArgLys(NBD)-OH (mGRK(NBD)-OH)

FIGURE 1: Structures of the titratable cationic vesicle-binding amphiphile mGH-edNBD and the zwitterionic vesicle-binding amphiphile mGRK(NBD)-OH. The ionized forms shown are the principal ones expected to be present when bound to a negatively charged lipid bilayer.

butoxycarbonyl-protected form and labeling the lysine ϵ-amino group with NBD-fluoride after deprotecting the completed acylpeptide. The final NBD-labeled products were stored (and added to vesicles) as 250 μM stock solutions in ethanol.

Large Unilamellar Vesicle Preparations. Lipid mixtures (3−10 μmol) were dried down under a stream of nitrogen at 45−55 °C from CH_2Cl_2/methanol (3:1) and further incubated under high vacuum for 4−6 h to remove residual traces of solvent. The dried lipids were dispersed in 0.5 mL of K^+- or Na^+-buffer (128 mM KCl or NaCl, respectively, 10 mM MOPS, 0.1 mM EDTA, titrated with KOH or NaOH to pH 7.4) by vortexing above the transition temperature, then five times freeze/thawed using ethanol/dry ice, and finally extruded 25 times through polycarbonate filters (pore size 0.1 μm unless otherwise indicated) using a hand-held extruder (*32*). Potassium-loaded vesicles in Na^+-buffer were prepared by passing vesicles prepared in K^+-buffer through a 10 mL column of Sephadex G-75 packed in Na^+-buffer. Vesicle lipid concentrations were quantitated by phosphorus determination (*26*).

Assays of Peptide Translocation. Lipid vesicles were incubated for varying times with labeled peptides, except where otherwise indicated, at lipid and peptide concentrations of 500 and 0.5 μM, respectively, at 37 °C and under argon with exclusion of light. Where indicated, valinomycin (from ethanolic solution, final ethanol concentration $\leq$0.2%) was added to the vesicles at a ratio of 1:200 000 mol/mol lipid. An equal level of ethanol was added to parallel samples incubated without valinomycin. We have shown previously (ref *33*; Skerjanc and Silvius, unpublished results; see also ref *34*) that in the presence of valinomycin, anionic lipid-containing vesicles such as those prepared here can develop a maximum transbilayer potential of −110 to −130 mV. For nearly all of the vesicle compositions and incubation conditions examined in this study, vesicle aggregation in the presence of peptides (as assessed by an increase in turbidity) was negligible or very limited. Addition of penetratin to vesicles combining phosphatidylcholine/phosphatidylethanolamine/cholesterol mixtures with phosphatidic acid, cardiolipin, or (particularly) lysobis-/semilysobis-phosphatidic acid led to a significant increase in vesicle turbidity. However, even in these latter cases, the vesicles remained well-dispersed throughout the course of the experiment.

The extent of internalization of NBD-labeled peptides into vesicles after incubation for various times was normally determined by dithionite reduction (*22*). Briefly, 200 μL aliquots of the vesicle/peptide incubation mixtures were injected into 2.8 mL of Na^+-buffer in a fluorometer cuvette with stirring at 37 °C, and 30 μL of 1 M freshly prepared sodium dithionite was then added while continuously recording the fluorescence (470/538 nm, slit widths 10/10 nm) in a Perkin-Elmer LS-50B luminescence spectrometer with a thermostated sample chamber. The percentage of NBD-labeled peptide internalized into the vesicles was determined from the fluorescence traces as illustrated in Figure 2B.

In an alternative assay for peptide internalization into vesicles, K^+-buffer-loaded donor lipid vesicles (combining neutral and anionic phospholipids) were first incubated with NBD- or bimane-labeled penetratin and valinomycin in Na^+-buffer at 37 °C as described previously. Aliquots of the incubation mixtures (200 μL) were injected into 2.8 mL of Na^+-buffer while continuously recording the fluorescence at 37 °C (470/538 nm [slit widths 10/10 nm] for NBD-labeled peptides or 390/468 nm [slidwidths 10/10 nm] for bimane-labeled peptides). A total of 5 μL of 5 mM sonicated DOPG acceptor vesicles, incorporating 2 mol % of Rho-PE or NBD-PE, was then added. Under these conditions, the more negatively charged DOPG acceptor vesicles rapidly bound (and hence quenched the fluorescence of) essentially all of the labeled peptide molecules remaining outside the donor vesicles at the moment of acceptor vesicle addition (a result confirmed by control experiments using varying concentrations of donor and acceptor vesicles under conditions in which peptide internalization was negligible). The percentage of labeled peptide uptake into donor vesicles was determined from the fluorescence data as described in the legend to Figure 5B.

Assays of Vesicle Contents Release and Lipid Mixing. Release of vesicle contents was determined by dequenching of the fluorescence of calcein entrapped at a self-quenching concentration (40 mM, combined with 5 mM Tes, 0.1 mM EDTA, 64 mM KCl) in vesicles. Calcein-loaded vesicles were incubated with or without penetratin and valinomycin as for the other assays described previously, and the extent of calcein release was determined by measuring the fluorescence (490/520 nm, slit widths 2.5/2.5 nm) before and after the addition of Triton X-100 (to 0.5%) to lyse the vesicles (*35*).

To assay lipid mixing between vesicles, two populations of K^+-buffer-loaded vesicles, one incorporating 1 mol % NBD-PE/0.5 mol % Rho-PE and the second unlabeled, were coincubated (at 100 and 400 μM vesicle lipid, respectively)

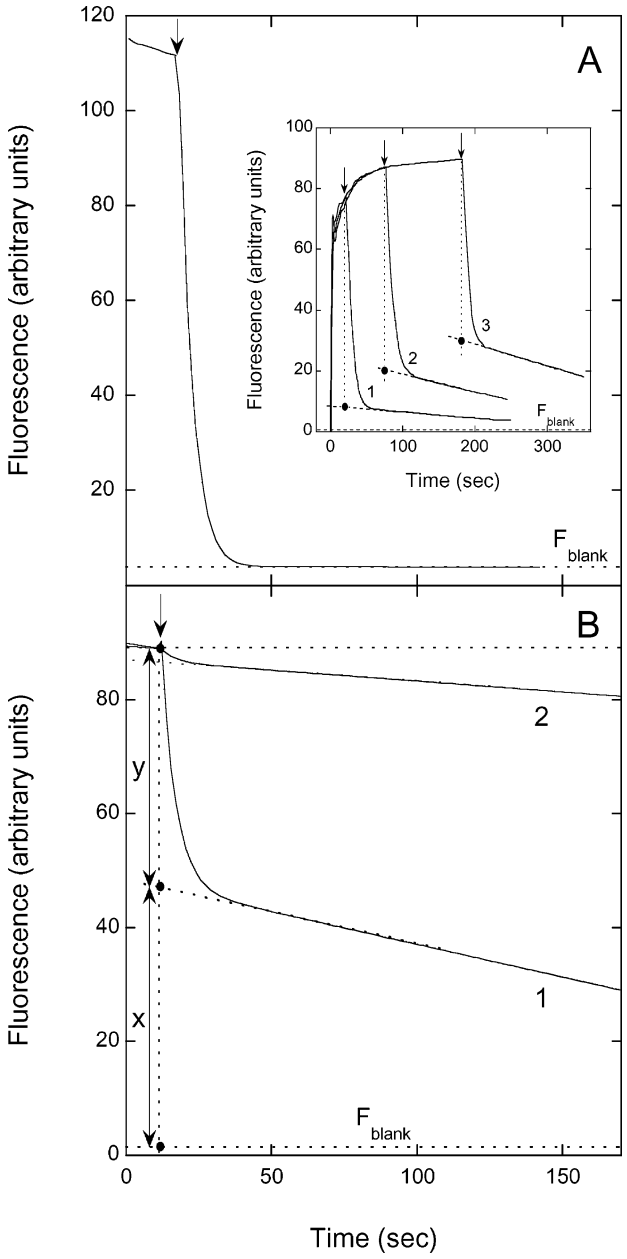

FIGURE 2: Panel A—Time course of dithionite reduction of NBD-labeled penetratin after preincubation of the peptide with DOPC/DOPG (3:1) vesicles (500 μM lipid, 0.5 μM peptide) for 30 min at 37 °C. A 200-μL aliquot of the preincubated peptide/vesicle mixture was injected into 2.8 mL of Na^+-buffer in the fluorometer cuvette at time zero. Subsequent addition of dithionite (10 mM, arrow) rapidly decreases the fluorescence signal to the baseline level measured for a control sample of vesicles without peptide (F_{blank}, dashed line), indicating negligible translocation of peptide into the vesicles. Inset—The titratable cationic probe mGH-edNBD was mixed with vesicles (100 μM lipid, 0.1 μM mGH-edNBD) in the fluorometer cuvette at time zero, and dithionite was added at a varying time thereafter (arrows—three separate traces are superimposed). The fraction of probe internalized rises with increasing time of probe-vesicle incubation prior to dithionite addition (note the increasing proportion of fluorescence that is protected from rapid quenching in curves 1, 2, and 3, respectively). Panel B—Time courses of dithionite reduction of mGH-edNBD after preincubation with DOPC/tetraoleoyl cardiolipin vesicles for 30 min at 37 °C. Curve 1—Incubation without a transbilayer potential gradient. The proportion of probe present inside the vesicles (= 100%(x/(x + y), where x and y are measured as indicated) is roughly 50%. Curve 2—Incubation with a transbilayer potential (+ valinomycin, inside negative); the proportion of probe present inside the vesicles increases to >95%.

in Na^+-buffer at 37 °C with or without bimane-labeled penetratin (0.5 μM) and valinomycin (1:200 000) mol/mol lipid). The fluorescence of diluted aliquots of the samples was then determined (wavelengths 470/538 nm, slit widths 10/10 nm) before and after adding Triton X-100 (to 1% w/v). The extent of lipid mixing was determined as described previously (*29*) from these two readings and parallel readings for control samples of vesicles with compositions corresponding to 0 and 100% lipid mixing in the previous mixtures.

Cell-Peptide Incubations and Fluorescence Microscopy. CV-1 or HeLa cells were grown to 80−90% confluency on glass cover slips in Dulbecco's minimum essential medium supplemented with 10% fetal bovine serum, 2 mM glutamine, and 50 μg/mL gentamycin. Cell monolayers were twice washed with serum-free medium, then incubated with Texas Red-labeled peptides (500 nM) in the same medium for varying times at 37 °C, and the live cells were imaged as described previously (*30*) on a Zeiss Axiovision 3.1 inverted fluorescence microscope through a 63X oil-immersion objective.

RESULTS

Peptide Translocation in Absence of a Transbilayer Potential. For most of the experiments described here, peptide internalization into vesicles was assayed by protection from externally added sodium dithionite (*13*, *22*, *36*). This charged reagent rapidly reduces (and thereby quenches the fluorescence of) NBD-labeled peptide molecules to which it has access, but it only very slowly diffuses across lipid bilayers. When a portion of the NBD-labeled peptide molecules in a given sample is present inside vesicles, the percentage of (blank-corrected) fluorescence that is resistant to rapid quenching by externally added dithionite is equal to the percentage of peptide molecules located within the vesicles (illustrated in Figure 2B). Except where otherwise noted, in the experiments described here using NBD-labeled penetratin (or NBD-labeled myristoyl-peptides), the peptide was essentially completely bound to lipid vesicles, as assessed (not shown) by measuring the binding-dependent enhancement of peptide fluorescence as a function of the vesicle concentration (*37*, *38*).

As shown in Figure 2A (main panel), after incubation with DOPC/DOPG (3:1 molar proportions)[2] large unilamellar vesicles for times up to several tens of minutes in the absence of a transbilayer potential, NBD-labeled penetratin remains essentially completely accessible to reduction by externally added dithionite, indicating negligible translocation of peptide under these conditions. Similar results were obtained for vesicles of several other lipid compositions tested (not shown).

To determine whether NBD-labeled penetratin can diffuse across lipid bilayers on longer time scales in the absence of a transbilayer potential, we incubated the labeled peptide with lipid vesicles of diverse compositions for 12 h at 37 °C, then determined the extent of peptide translocation using the dithionite assay. As summarized in the second column of Table 1, in the absence of a transbilayer potential, vesicles of a wide variety of compositions show very limited

[2] All lipid compositions in this paper are specified as molar proportions.

Table 1: Uptake of NBD-Labeled Penetratin into Large Unilamellar Vesicles of Various Compositions in the Presence or Absence of a Transmembrane Potential

vesicle composition[b]	peptide uptake in 12 h[a]: −valinomycin	+valinomycin	maintenance of $\Delta\Psi$[c]
POPC/POPA (3:1)	0.2 ± 0.1	1.9 ± 0.2	+++
POPC/POPE/POPA (3:3:2)	0.1 ± 0.1	4.4 ± 0.2	++
DOPC/DOPA (3:1)	0.6 ± 0.1	0.3 ± 0.2	++
POPC/POPE/POPA/Chol (3:3:2:4)	0.6 ± 0.2	3.3 ± 0.3	++
DOPC/DOPE/DOPA (3:3:2)	1.4 ± 0.5	9.9 ± 0.7	+
DOPC/DOPE/DOPA/Chol (3:3:2:4)	1.0 ± 0.1	24.4 ± 1.5	+
DOPC/CL (7:1)	0.7 ± 0.2	2.3 ± 0.4	++
DOPC/DOPE/CL (3:3:2)	1.4 ± 0.4	11.5 ± 0.7	++
DOPC/DOPE/CL/Chol (3:3:2)	8.0 ± 0.2	21.9 ± 0.5	++
POPC/LBPA/SLBPA (6:1:1)	0.4 ± 0.1	24.2 ± 1.6	+++
DOPC/LBPA/SLBPA (6:1:1)	1.6 ± 0.3	12.5 ± 2.7	++
DOPC/DOPE/LBPA /SLBPA/Chol (3:3:1:1:4)	9.2 ± 2.1	17.0 ± 7.0	+
POPC/LBPA (3:1)	1.1 ± 0.1	33.0 ± 1.4	+++
DOPC/LBPA (3:1)	4.0 ± 0.9	17.4 ± 6.5	++
POPC/POPS (3:1)	0.6 ± 0.1	54.5 ± 2.9	+++
POPC/POPE/POPS (3:3:2)	0.4 ± 0.2	15.9 ± 0.7	+++
ePC/ePE/DOPS (3:3:2)	1.7 ± 0.3	5.8 ± 0.6	+++
DOPC/DOPS (3:1)	1.7 ± 0.4	6.5 ± 3.4	++
POPC/POPE/POPS/Chol (3:3:2:4)	0.6 ± 0.1	6.0 ± 0.3	++
ePC/ePE/DOPS/Chol (3:3:2:4)	0.9 ± 0.1	6.4 ± 0.3	+++
DOPC/DOPE/DOPS (3:3:2)	2.1 ± 0.5	8.8 ± 0.4	++
DOPC/DOPE/DOPS/Chol (3:3:2:4)	1.1 ± 0.1	8.9 ± 0.2	++
POPC/POPG (1:1)	3.7 ± 0.3	58.7 ± 1.7	+++
POPC/POPG (3:1)	1.7 ± 0.4	22.4 ± 0.2	+++
DOPC/DOPG (1:1)	1.4 ± 0.1	21.2 ± 3.0	+++
DOPC/DOPG (3:1)	0.8 ± 0.4	10.2 ± 0.2	++
DOPC/DOPE/DOPG (3:3:2)	2.0 ± 0.5	3.3 ± 0.9	++
DOPC/DOPE/DOPG/Chol (3:3:2:4)	0.9 ± 0.1	9.4 ± 0.4	+
POPC/soy PI (3:1)	2.5 ± 0.4	71.9 ± 4.6	++
ePC/soy PI (3:1)	1.7 ± 0.2	64.9 ± 0.5	+++
DOPC/soy PI (3:1)	7.5 ± 3.2	30.7 ± 6.8	++
POPC/soy PI/Chol (3:1:2)	0.8 ± 0.1	27.1 ± 5.9	+++
ePC/soy PI/Chol (3:1:2)	0.4 ± 0.2	30.2 ± 0.8	+++
DOPC/soy PI/Chol (3:1:2)	0.1 ± 0.1	9.9 ± 0.2	+++
DOPC/DOPE/soy PI/Chol (3:3:2:4)	1.1 ± 0.3	7.0 ± 0.6	++
soybean asolectin[d]	1.5 ± 0.4	3.2 ± 0.3	+
POPC/PI + PI-phosphates (3:1)	13.4 ± 4.3	28.7 ± 0.6	++
DOPC/PI + PI-phosphates (3:1)	4.2 ± 0.2	14.7 ± 1.7	++
ePC/SM/Gang/Chol (95:95:10:100)	1.3 ± 0.5	9.8 ± 2.3	++
ePC/SM/Sulf/Gang/Chol (85:85:20:10:100)	2.6 ± 1.7	30.1 ± 6.2	++

[a] Vesicles of the indicated compositions (500 μM lipid), loaded with K^+-buffer and suspended in Na^+-buffer, were incubated for 12 h with NBD-labeled penetratin (0.5 mM) at 37 °C under argon and with exclusion of light. The percentage of added peptide taken up by the vesicles was then determined by the dithionite assay as discussed in the text. Data shown represent the average (±SD) of duplicate or triplicate determinations in each of at least two independent experiments. [b] Special abbreviations used: CL, tetraoleoyl cardiolipin; LBPA, dioleoyl-lysobisphosphatidic acid; SLBPA, trioleoyl-semilysobisphosphatidic acid; Chol, cholesterol; ePC, egg yolk phosphatidylcholine; PI + PI-phosphates, yeast-derived fraction composed of PI plus approximately 20% PI-mono- and diphosphates; SM, bovine brain sphingomyelin; Gang, mixed brain gangliosides; Sulf, brain sulfatide. [c] Determined from the maintenance of accumulation of mGH-edNBD inside vesicles over time in the presence of valinomycin and bimane-labeled penetratin as described in the text. The results of these measurements are summarized as follows: +++: maintains >90% internalization of the probe for >6 h; ++: maintains >80% internalization of the probe for >6h; +: shows <80% (typically, <70%) internalization of the probe by 6 h. [d] Major lipid components comprise approximately 45% polyunsaturated phosphatidylcholine, 30% polyunsaturated phosphatidylethanolamine, and 20% polyunsaturated phosphatidylinositol.

internalization of NBD-labeled peptide even after this extended incubation. As noted previously, for almost all the lipid compositions tested (with the noteworthy exceptions of PC/sphingomyelin/ganglioside/cholesterol and PC/sphingomyelin/sulfatide/ganglioside/cholesterol vesicles), virtually all of the labeled peptide was vesicle-bound at the lipid concentration used in these experiments (500 μM), in agreement with previously reported conclusions for similar systems (*38*, *39*). When no potential gradient is present, roughly 50% of the peptide therefore should accumulate inside the vesicles at equilibrium. It is thus apparent that in the absence of a transbilayer potential, transbilayer movement of the labeled penetratin peptide is very slow (<1%/h) for vesicles of diverse compositions. LUV with several lipid compositions tested (including soybean asolectin, DOPC/DOPG, DOPC/DOPS, and ePC/tPE/DOPS/cholesterol) gave very similar results when prepared by extrusion through 0.4 μm rather than 0.1 μm pore-diameter filters (not shown).

As a positive control for the previous experiments, we incubated replicate portions of vesicles with the fluorescent-

labeled vesicle-binding probe mGH-edNBD (see Figure 1), which like other titratable cationic amphiphiles (*40*) can permeate across the bilayer in its unprotonated form. As shown in the inset to Figure 2A, after addition to the vesicles, an increasing proportion of this species becomes protected from dithionite reduction over a period of several minutes. After preincubation with vesicles for 30 min, the internal (protected) fraction reaches the level of ca. 50% expected for a random distribution of probe molecules between the inner and the outer vesicle leaflets (Figure 2B, curve 1). It is thus evident that the dithionite assay can faithfully detect transbilayer movement of NBD-labeled peptides.

Potential-Driven Penetratin Translocation—Effects of Lipid Composition. The lipid vesicles used in the experiments summarized in Table 1 were prepared with K^+-buffer internally and Na^+-buffer externally, permitting the development of a transbilayer potential (inside negative) upon the addition of valinomycin (1:200 000 mol/mol lipid). The results of measurements of the uptake of penetratin into such vesicles after an extended incubation (12 h at 37 °C) in the presence of valinomycin are summarized in the third column of Table 1. For most of the vesicle compositions tested, imposition of a transbilayer potential substantially enhances the internalization of labeled penetratin during such incubations, in some cases to levels exceeding 50% of total peptide. Comparable results were found for vesicles of several compositions (including DOPC/DOPG, DOPC/soy PI, POPC/soy PI, or POPC/POPS [3:1]) when the incubations were carried out at pH 6.0 or 6.5 instead of 7.4 and when the peptide concentration was decreased 3-fold at a fixed lipid concentration (see example in Figure 4B). Importantly, in parallel experiments using vesicles prepared with internal and external Na^+-buffer (including vesicles with all of the lipid compositions that gave ≥25% uptake of penetratin in the presence of valinomycin in the experiments summarized in Table 1), no significant enhancement of penetratin internalization was observed in the presence versus the absence of valinomycin (not shown). This result indicates that a transmembrane potential, and not the presence of valinomycin per se, was required to enhance the translocation of peptide into vesicles.

From the data shown in Table 1, it is evident that the different types of lipid vesicles examined vary widely in their ability to internalize penetratin during an extended incubation with the peptide and valinomycin. In principle, these differences could reflect not only intrinsic effects of lipid composition on peptide translocation efficiency but also variations in the abilities of vesicles with different compositions to maintain a transbilayer potential during the prolonged incubation period. To assess the effects of this latter factor on the results listed in Table 1, we measured the potential-dependent internalization of the titratable cationic amphiphile mGH-edNBD by the different types of vesicles under analogous conditions.

As discussed previously (see, e.g., refs *40* and *41*), lipid vesicles can internalize titratable cationic amphiphiles such as mGH-edNBD to concentrations much higher than the extravesicular level when a transbilayer potential (inside negative) is imposed, as a consequence of the transmembrane potential, and to a lesser degree, the creation of an attendant pH gradient. This behavior is illustrated in Figure 2B, where within 30 min of the addition of valinomycin to mGH-edNBD-labeled lipid vesicles (6:1 DOPC/cardiolipin in the example shown) the level of accumulation of the probe within the vesicles, assayed by dithionite reduction as described previously, increases from 50 to >95%. As illustrated in Figure 3A,B for vesicles of several compositions, the extent of internalization of mGH-edNBD subsequently decays over time, at a rate that varies markedly with lipid composition and that is only modestly enhanced in the presence of bimane-labeled penetratin (which as demonstrated later interacts with vesicles in a manner very similar to the NBD-labeled peptide). This assay proved most suitable to examine the maintenance of the transbilayer potential in large numbers of samples under the conditions used to measure penetratin translocation. However, the results of parallel experiments using the potential-sensitive fluorescent dye $diSC_3(5)$ (*42*) led to similar conclusions concerning the abilities of different types of vesicles to maintain a transbilayer potential. In Table 1 (final column), we compare the abilities of vesicles of different compositions to maintain a transbilayer potential over time in the presence of valinomycin and (bimane-labeled) penetratin.

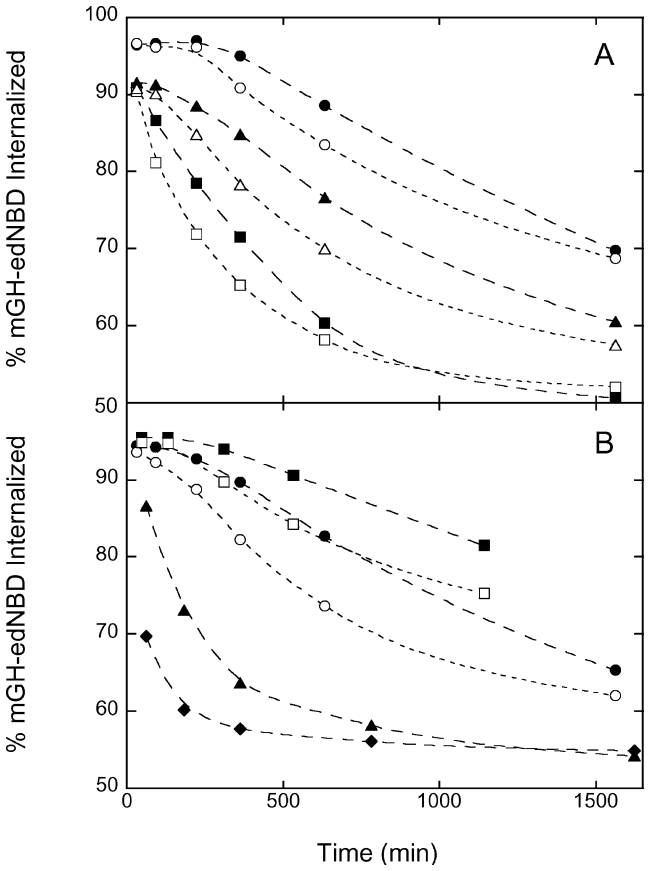

FIGURE 3: Time courses of internalization of mGH-edNBD by K^+-buffer-loaded lipid vesicles in Na^+-buffer in the presence of valinomycin alone (filled symbols) or valinomycin and bimane-labeled penetratin (open symbols). Incubation mixtures contained lipid (500 μM), mGH-edNBD (0.5 μM), and valinomycin (1:200 000 mol/mol lipid) with or without 0.5 μM penetratin (filled and open symbols, respectively). Internalization of mGH-edNBD by vesicles after incubation for the indicated times at 37 °C was measured as described in the text and as illustrated in Figure 2B. Panel A—(●,○) DOPC/tetraoleoyl cardiolipin (6:1); (▲,△) DOPC/DOPA (3:1); or (■/□) DOPC/DOPE/DOPA (3:3:2) vesicles. Panel B—(■/□) POPC/soy PI (3:1), (●,○) DOPC/DOPG (3:1), (▲) soybean asolectin, or (◆) DOPC/DOPE/DOPA/cholesterol (3:3:2:4) vesicles.

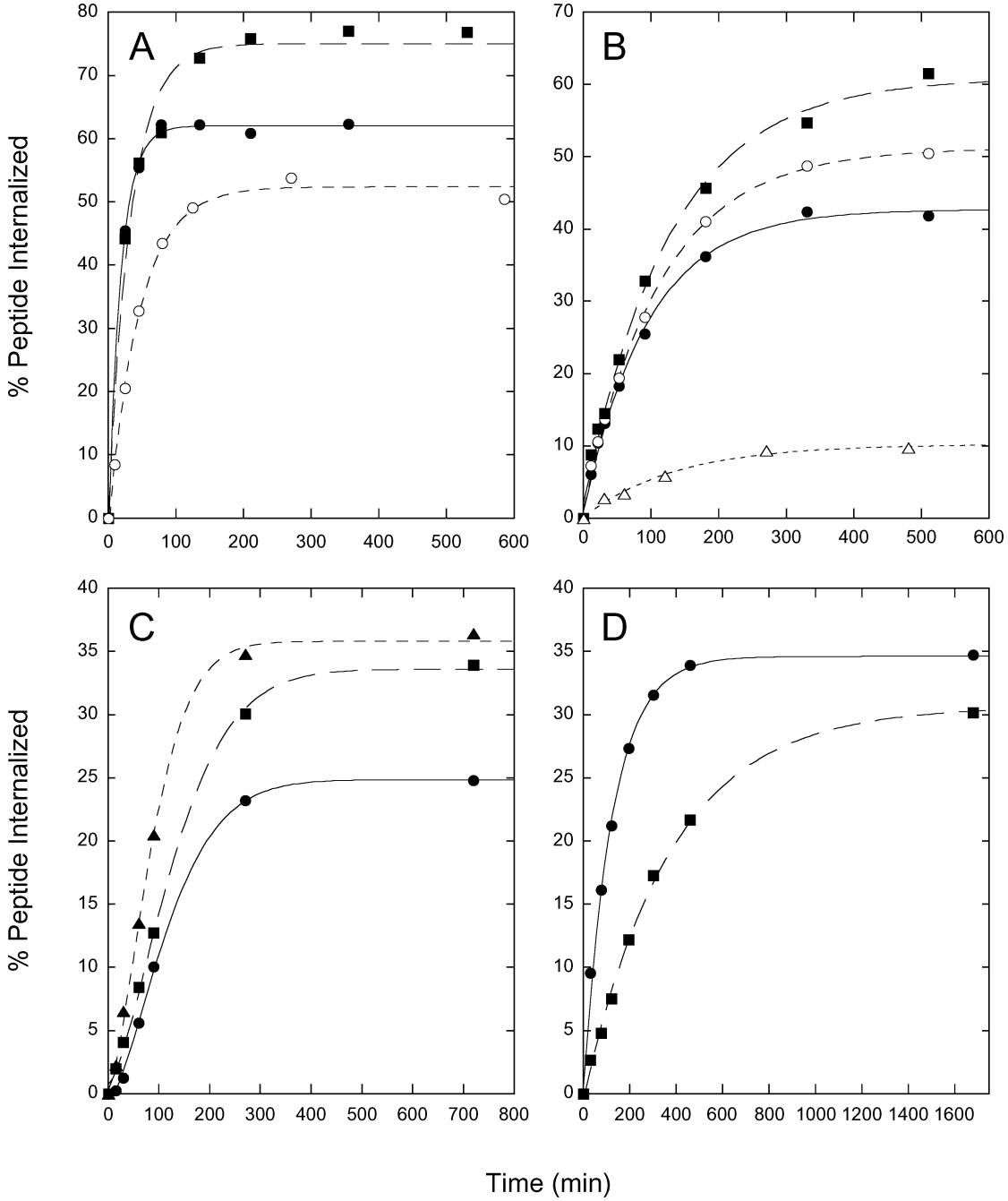

FIGURE 4: Time courses of uptake of NBD-labeled cationic peptides into lipid vesicles in the presence of a transbilayer potential. Peptides were incubated with K^+-buffer-loaded vesicles in Na^+-buffer in the presence of valinomycin for the indicated times, and the uptake of peptide into the vesicles was then assayed by protection from dithionite reduction. Panel A—POPC/soy PI vesicles incubated with (●) penetratin or (■) R_6GC-NH_2 or (○) POPC/POPS vesicles incubated with penetratin. Panel B—DOPC/soy PI (3:1) vesicles incubated with (●) penetratin, (○) penetratin at 0.16 μM rather than the normal 0.5 μM, (■) R_6GC-NH_2, or (△) mGRK(NBD)-OH. Panel C—DOPC/DOPE/DOPA/cholesterol (3:3:2:4) vesicles incubated with (●) penetratin, (■) R_6GC-NH_2, or (▲) K_6GC-NH_2. Panel D—ePC/sphingomyelin/ganglioside/sulfatide/cholesterol (85:85:10:20:100) vesicles incubated with (●) penetratin or (■)R_6GC-NH_2. Other experimental conditions were as described in the text.

Combining the results of our measurements of penetratin translocation and of maintenance of a potential gradient for lipid vesicles of various compositions (Table 1, third and fourth columns), we can conclude that the efficiency of potential-dependent transbilayer uptake of penetratin is strongly dependent on the bilayer lipid composition. To facilitate analysis of the data shown in Table 1, the vesicle lipid compositions have been organized into blocks, where all compositions within a given block include the same anionic lipid (e.g., phosphatidic acid, regardless of acyl chain composition), and within each block the compositions are arranged in order of increasing estimated proclivity to form inverted nonlamellar phases (increasing as acyl chain unsaturation, and content of phosphatidylethanolamine and/or cholesterol, increase (*43*−*45*)). The blocks of data are in turn ordered in terms of increasing size of the anionic lipid headgroup, from phosphatidic acid (smallest) to gangliosides (largest).

From the results presented in Table 1, two patterns of dependence of the efficiency of penetratin translocation on lipid composition can be discerned. First, for vesicles containing anionic lipids with small headgroups (e.g., phos-

Table 2: Extents and Initial Rates of Internalization of Polybasic Peptides by Lipid Vesicles at 37°C

vesicle composition[b]	peptide	peptide uptake in 12 h[a]: −valinomycin	+valinomycin	initial rate of uptake (%/h)[c]
DOPC/DOPE/DOPA (3:3:2)	Pen	1.4 ± 0.2	9.9 ± 0.7	ND
	R_6	0.8 ± 1.1	19.1 ± 1.1	ND
	K_6	1.8± 0.2	29.6 ± 2.2	ND
DOPC/DOPE/DOPA/Chol (3:3:2:4)	Pen	1.0 ± 0.1	26.2 ± 1.3	14 ± 1
	R_6	1.3 ± 1.1	34.9 ± 1.1	21 ± 2
	K_6	2.0 ± 0.5	36.2 ± 1.6	34 ±1
DOPC/LBPA/SLBPA (6:1:1)	Pen	1.4 ± 0.6	21.2 ± 3.0	23.4 ± 3.1
	R_6	1.3 ± 0.2	18.6 ± 5.1	52 ± 14
	K_6	1.0 ± 0.1	21.9 ± 3.7	62 ± 13
DOPC/DOPE/LBPA/SLBPA/Chol (3/3/1/1:4)	Pen	9.2 ± 4.2	29.3 ± 0.7	ND
	R_6	52.8 ± 3.6	55.4 ± 4.4	ND
	K_6	53.6 ± 1.1	64.1 ± 5.1	ND
DOPC/DOPG (1:1)	Pen	1.2 ± 0.1	19.6 ± 3.5	20 ± 4
	R_6	2.4 ± 1.1	7.2 ± 1.9	1.4 ± 0.4
	K_6	3.2 ± 0.1	8.9 ± 2.3	2.8 ± 0.9
POPC/POPS (3:1)	Pen	0.6 ± 0.1	55.1 ± 2.7	117 ± 13
ePC/tPE/DOPS (3:3:2)	Pen	0.9 ± 0.1	6.4 ± 0.4	ND
	R_6	5.4 ± 0.2	29.5 ± 0.8	ND
	K_6	5.9 ± 0.3	31.0 ± 1.7	ND
POPC/Soy PI (3:1)	Pen	5.1 ± 3.7	66.4 ± 4.7	243 ± 73
	R_6	6.3 ± 2.7	79.8 ± 5.6	218 ± 26
DOPC/Soy PI (3:1)	Pen	3.1 ± 0.4	26.8 ± 7.1	43 ± 12
	R_6	10.1 ± 1.7	52.8 ± 10.2	46 ± 10
POPC/PI + PI-phosphates (3:1)	Pen	13.4 ± 4.3	28.9 ± 0.2	91 ± 6
ePC/SM/Gang/Sulf/Chol (85:85:10:20:100)	Pen	2.3 ± 0.6	34.8 ± 1.7	28 ± 2
	R_6	3.1 ± 0.8	25.2 ± 2.2	8.2 ± 1.0

[a] Vesicles were incubated with NBD-labeled penetratin, R_6GC-NH_2, or K_6GC-NH_2 for 12 h at 37 °C, and the percentage of peptide internalized was then determined using the dithionite-reduction assay, as described for Table 1. Values indicated for penetratin were averaged only from experiments in which penetratin was examined along with the other peptides indicated and hence may differ from the analogous values listed in Table 1. [b] Special abbreviations for lipids are as indicated in footnote a for Table 1. The NBD-labeled peptides penetratin, R_6GC-NH_2, and K_6GC-NH_2 are abbreviated respectively as Pen, R_6, and K_6. [c] Initial rates were determined by fitting time courses such as those shown in Figure 4 to an equation of the form $f(t) = A - B\exp(-kt)$ with A, B, and k as adjustable parameters; the initial slope was calculated from the fitted values as (kB). Values shown represent the average (±half-range) of duplicate determinations. ND—not determined.

phatidic acid and cardiolipin), the efficiency of potential-dependent peptide internalization increases as the inverted phase-forming proclivity of the lipid mixture increases. Second, and in distinct contrast, for vesicles containing anionic lipids with relatively large headgroups (e.g., phosphatidylinositol and phosphatidylserine), the efficiency of peptide translocation decreases as the inverted phase-forming tendency of the lipid mixture increases. These trends can be discerned even after factoring out the abilities of different types of vesicles to maintain a transbilayer potential for extended times. Thus, for example, POPC/POPA vesicles show much poorer uptake of labeled penetratin than do DOPC/DOPE/DOPA/cholesterol vesicles (ca. 2% vs 24%, respectively) in the presence of valinomycin, even though the former vesicles maintain a potential gradient much better under these conditions than do the latter. Conversely, POPC/soy PI vesicles show much greater uptake of peptide in the presence of valinomycin than do DOPC/soy PI/cholesterol vesicles (ca. 72% vs 10%, respectively), even though the latter vesicles better maintain their transbilayer potential under these conditions. It is thus apparent that the features of lipid composition noted previously can directly influence the ability of penetratin to translocate across lipid bilayers, independently of effects on the abilities of different vesicles to maintain a substantial transbilayer potential during prolonged incubations.

As the final set of entries in Table 1 indicates, vesicles combining neutral and anionic sphingolipids with phosphatidylcholine and cholesterol show significant uptake of NBD-labeled penetratin in the presence of a transbilayer potential. This finding is noteworthy in view of the fact that these lipid compositions mimic that of the extracytoplasmic leaflet of the plasma membrane and (most probably) of early endocytic vesicles, which are the membrane compartments with which penetratin will associate early in its interaction with mammalian cells.

Time Courses of Potential-Dependent Peptide Uptake. We next examined in more detail the time courses of potential-dependent uptake of labeled penetratin into lipid vesicles with compositions that supported significant peptide translocation in the previous experiments. Results from these experiments are illustrated in Figure 4 and summarized in Table 2, where we also include data obtained using the NBD-labeled peptides R_6GC-NH_2 and K_6GC-NH_2, which carry the same number of basic residues as penetratin. These data illustrate two noteworthy points. First, in the presence of a transbilayer potential, all three peptides can exhibit significant rates of uptake into vesicles of diverse lipid compositions. (The rate indicated for internalization of penetratin into phosphatidylcholine/sphingomyelin/sulfatide/ganglioside/cholesterol vesicles is in fact likely to be strongly underestimated relative to the other rates tabulated since as noted previously, peptide binding to vesicles of this composition was relatively weak under our assay conditions.) The rate of peptide uptake into vesicles was not strongly dependent on the peptide concentration, as illustrated in Figure 4B.

A second noteworthy feature of the time courses of potential-dependent peptide uptake into vesicles is that the

rate of internalization typically falls off markedly over time, while the level of internal accumulation is still well below 100% or in some cases even below 50%, the equilibrium level expected in the absence of a transbilayer potential. This behavior may reflect the gradual decay of the transbilayer potential with time, as demonstrated previously. Consistent with this suggestion, adding increasing concentrations of extravesicular potassium to reduce the transbilayer potential progressively reduces the initial rate of peptide internalization into POPC/soy PI (3:1) vesicles (Figure 5A) or POPC/POPS (3:1) vesicles (not shown). Interestingly, however, there is no indication that the rate of translocation declines abruptly as the imposed transbilayer potential falls below some critical threshold value.

To corroborate our conclusion that penetratin can exhibit efficient time- and potential-dependent uptake into lipid vesicles, we also employed an alternative assay to assess this process, using either NBD- or bimane-labeled penetratin. In this assay, donor vesicles, combining neutral and anionic lipids, loaded with K^+-buffer and suspended in Na^+-buffer are first incubated with labeled peptide and valinomycin in the usual manner. Diluted aliquots of the incubation mixture are then mixed with DOPG acceptor vesicles containing one of the energy-transfer quenchers Rho-PE (for NBD-labeled penetratin) or NBD-PE (for bimane-labeled penetratin) while continuously recording the fluorescence. As illustrated in the inset to Figure 5B, the extent of fluorescence quenching observed upon addition of the acceptor vesicles, which exhibit much higher affinity for polybasic peptides than do the less strongly charged donor vesicles (*37*, *39*, *46*), provides a measure of the fraction of peptide that has been internalized by the donor vesicles (see Figure 5B inset). In Figure 5B, we plot the time course of internalization of NBD- or bimane-labeled penetratin, determined in this manner for samples of peptide incubated with POPC/POPS (3/1) donor vesicles. The two labeled peptides accumulate to similar extents inside the donor vesicles, with similar kinetics of uptake. The time course of uptake of NBD-labeled penetratin into the POPC/POPS vesicles is very similar to that determined using the dithionite-reduction assay (Figure 5B, open vs closed circles).

Assays of Peptide-Induced Vesicle Destabilization. Peptide internalization into lipid vesicles could in principle be accompanied and/or triggered by a large-scale loss of vesicle integrity. To test this possibility, vesicles were prepared loaded with calcein in an isoosmotic potassium-based buffer, and release of vesicle contents was monitored by dequenching of calcein fluorescence (*35*) in the absence or presence of penetratin and valinomycin. Representative results are shown in Figure 6A,B, illustrating experiments using POPC/POPS (3:1) and DOPC/DOPE/DOPA/cholesterol (3:3:2:4) vesicles, respectively. Leakage of vesicle contents in the absence of peptide and valinomycin is very slow in both cases (<1%/h) and is only modestly enhanced (remaining below 2%/h) in the presence of valinomycin and either bimane- or NBD-labeled peptide. The rate of vesicle contents leakage in the presence of penetratin and valinomycin is thus much lower than that of penetratin uptake into vesicles of the same compositions (upper curves, Figure 6A,B). Similar results were obtained for POPC/soy PI (3:1) and DOPC/DOPG (1:1) vesicles in analogous experiments (not shown). It should be noted that for the LUV preparations employed here (with mean diameters of ca. 100−110 nm), roughly 100

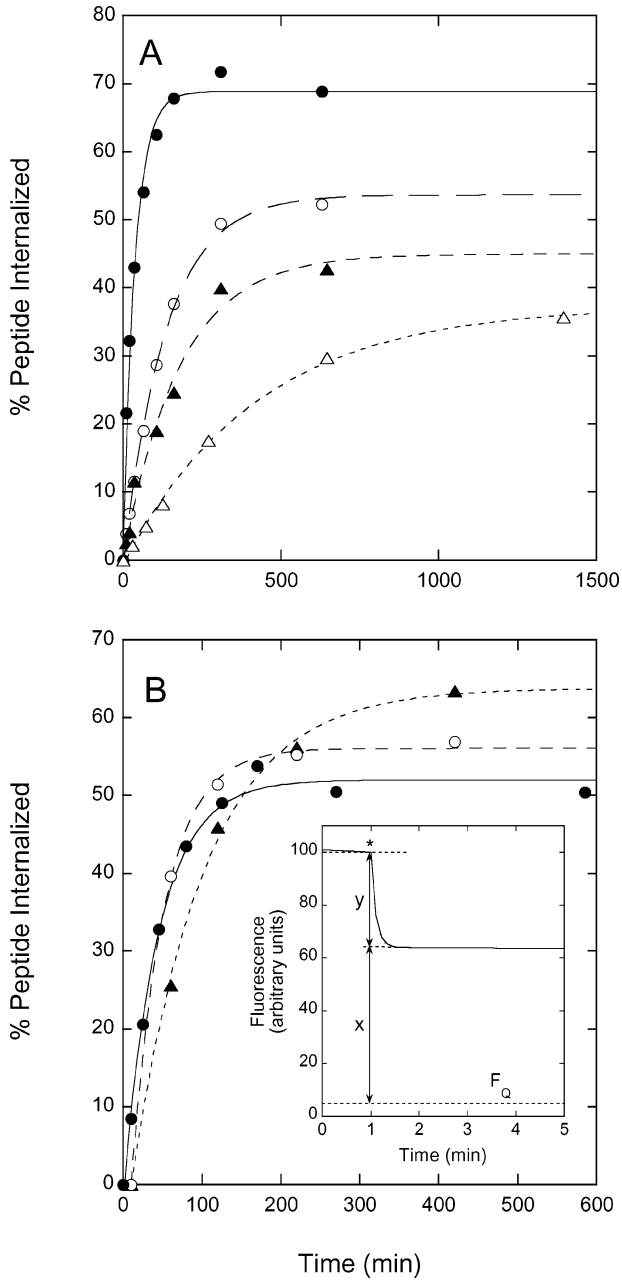

FIGURE 5: Panel A—Time courses of uptake of NBD-labeled penetratin, determined as described for Figure 4, into K^+-buffer-loaded POPC/POPS (3:1) vesicles incubated with peptide and valinomycin in Na^+-buffer containing (●) no KCl, (○) 1.92 mM KCl, (▲) 3.84 mM KCl, or (△) 12.8 mM KCl. The maximum theoretical transbilayer potentials that can be generated in the latter three incubations are −113, −94, and −62 mV, respectively. In a parallel run, a valinomycin-treated sample of POPC/POPS (3:1) vesicles prepared with Na^+-buffer internally and externally showed 0.9% internalization of penetratin after incubation for 24 h. Panel B—Time courses of uptake of (○) NBD- and (▲) bimane-labeled penetratin into POPC/POPS (3:1) donor vesicles, assayed by the energy transfer-based procedure described in the text. The time course of uptake of NBD-labeled penetratin into vesicles of the same composition, as determined using the dithionite assay (●), is shown for comparison. Panel B inset—Sample time course illustrating data analysis for the energy transfer-based assay of peptide translocation (F_Q = fluorescence of an identical quantity of peptide entirely bound to acceptor vesicles). At the asterisk, acceptor vesicles (DOPG + 2% NBD-PE or Rho-PE) are added to a preincubated sample of donor vesicles and peptide. From the resulting rapid decrease in fluorescence, the percentage of peptide internalized into the vesicles is calculated as $100\%(x/(x + y))$, where x and y are measured as shown.

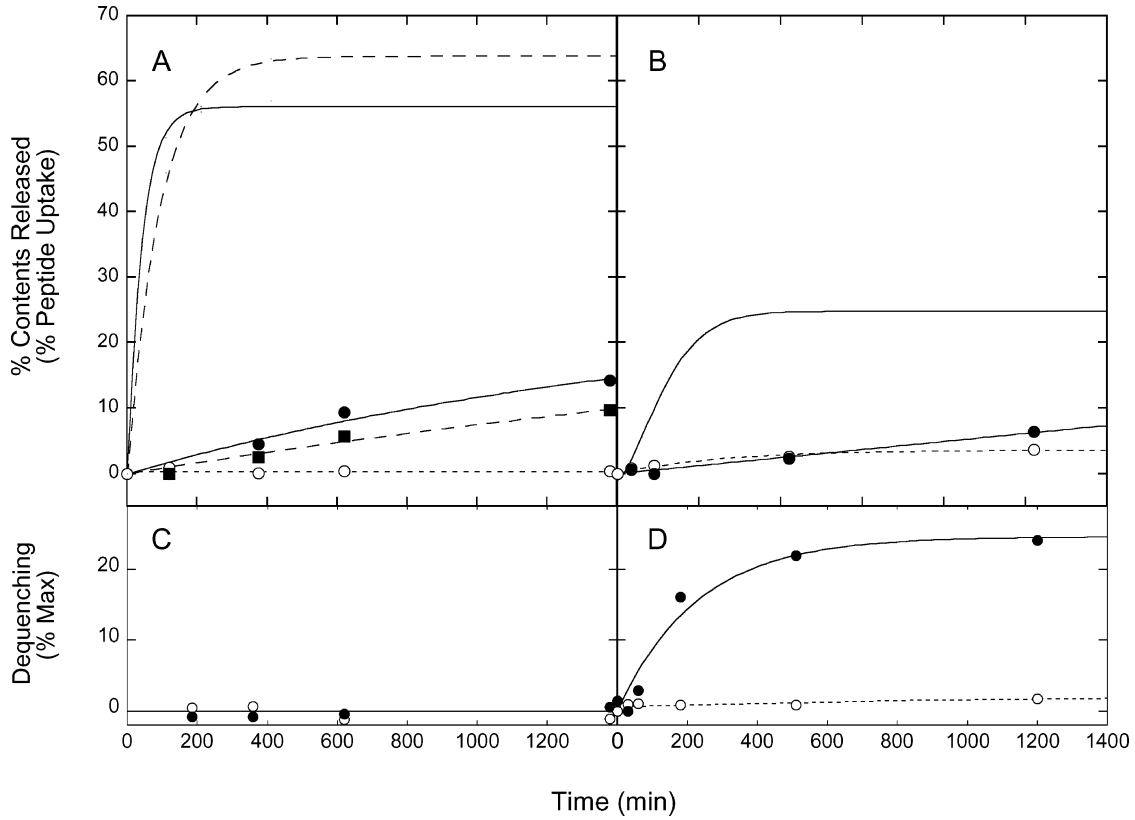

FIGURE 6: Time courses of lipid mixing and leakage for K^+-buffer-loaded lipid vesicles incubated with or without penetratin and valinomycin in Na^+-buffer. Panel A—Leakage of contents (assayed as calcein release) from POPC/POPS (3:1) vesicles with (○) no additions, (●) NBD-labeled penetratin and valinomycin added, or (■) bimane-labeled penetratin and valinomycin added. For comparison, the time courses determined for potential-dependent uptake of penetratin into vesicles of the same composition (Figure 5B) are also shown (solid curve without symbols—NBD-labeled penetratin; dashed curve without symbols—bimane-labeled penetratin). Panel B—Leakage of contents from DOPC/DOPE/DOPA/cholesterol (3/3/2/4) vesicles with (○) no additions or (●) NBD-labeled penetratin and valinomycin added. Upper solid curve without symbols—time course of potential-dependent uptake of NBD-labeled penetratin into vesicles of the same composition (from Figure 4C). Panel C—Lipid mixing between POPC/POPS (3:1) vesicles with (○) no additions or (●) bimane-labeled penetratin and valinomycin added. Panel D—Lipid mixing between DOPC/DOPE/DOPA/cholesterol (3:3:2:4) vesicles with (○) no additions or (●) bimane-labeled penetratin and valinomycin added. Other experimental conditions were as described in the text.

peptide molecules are present per vesicle in a standard incubation mixture. It is thus evident that individual peptide-translocation events are not accompanied by a large-scale loss of bilayer integrity.

To corroborate our conclusion that leakage of contents is modest under conditions of peptide uptake into vesicles, for vesicles of several compositions we also examined the rate of internalization of the zwitterionic vesicle-binding probe mGRK(NBD)-OH (structure shown in Figure 1) in the presence of bimane-labeled penetratin and valinomycin. This probe showed only slow and limited uptake into vesicles under conditions where the rate and extent of uptake of penetratin translocation were much greater, as illustrated in Figure 4B for POPC/soy PI (3:1) vesicles and as observed as well for POPC/POPS (3:1), DOPC/DOPG (1:1), and DOPC/dioleoyl-lysobisPA/trioleoyl-semilysobisPA (6:1:1) vesicles (not shown). These results support the conclusion from our calcein-leakage measurements that potential-dependent internalization of labeled penetratin into lipid vesicles can proceed without a substantial loss of overall bilayer integrity.

Assays of Peptide-Induced Intervesicle Lipid Mixing. To determine whether internalization of peptides by lipid vesicles is accompanied by vesicle fusion or hemifusion, using the NBD-PE/rhodaminyl-PE dequenching assay (*29*) we examined the ability of penetratin to promote lipid mixing between several types of vesicles that exhibited significant internalization of the peptide. Results from some representative experiments are shown in Figure 6C,D. Two distinct patterns of behavior are observed. For vesicles composed of POPC and POPS (Figure 6C), as well as for DOPC/DOPG (1:1 or 3:1) and POPC/soybean PI (3:1) vesicles (not shown), negligible lipid mixing is observed in the presence of peptide and valinomycin, even on time scales substantially longer than those required for peptide internalization. By contrast, for vesicles composed of DOPC/DOPE/DOPA/cholesterol (3:3:2:4), incubation with bimane-labeled peptide and valinomycin leads to substantial lipid mixing on a time scale of a few hours, while lipid mixing is negligible in the absence of peptide and ionophore (Figure 6D). Significant lipid mixing in the presence of valinomycin and penetratin was also observed for DOPC/DOPE/tetraoleoyl cardiolipin/cholesterol (3:3:1:4) and DOPC/dioleoyl-lysobisPA/trioleoyl-semilysobisPA (6:1:1) vesicles (not shown).

Cellular Uptake of Fluorescent Polycationic Peptides. In a final series of experiments, we examined the interactions of penetratin, R_6GC-NH_2, and K_6GC-NH_2 with living mammalian cells. After short times of incubation of CV-1 or HeLa cells with Texas Red-labeled penetratin, fluorescence is observed mainly in vesicular compartments (Figure

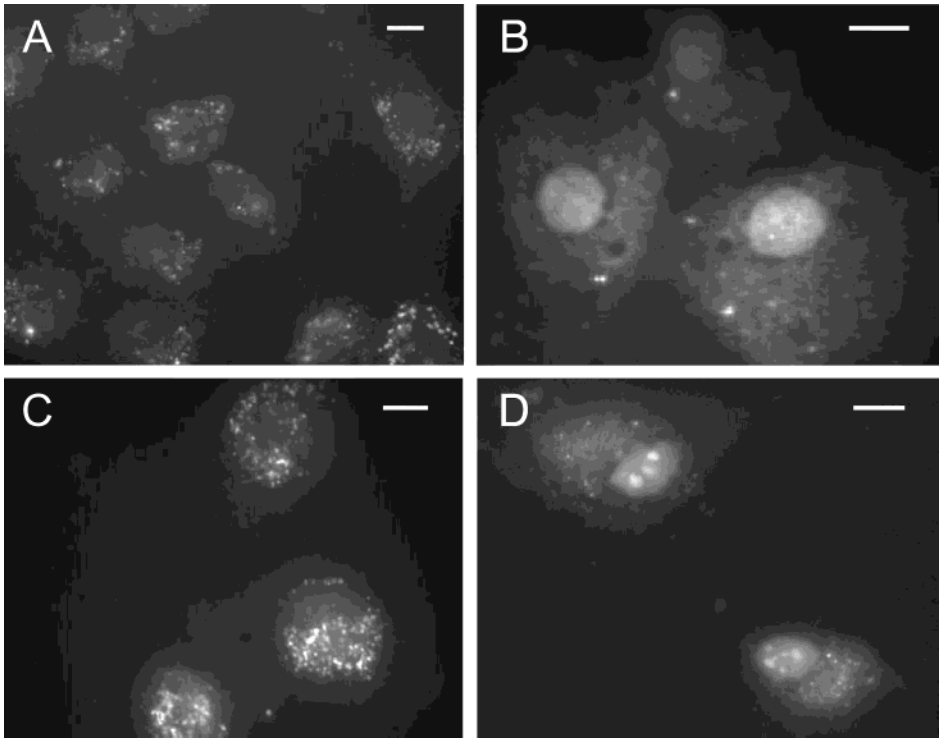

FIGURE 7: Fluorescence micrographs of living cultured cells incubated with Texas Red-labeled cationic peptides (500 μM) in serum-free medium at 37 °C. Panels A and B—CV-1 cells incubated for 30 min or 4 h, respectively, with labeled penetratin. Panels C and D—HeLa cells incubated for 1 or 4 h, respectively, with labeled penetratin.

7A,C). After incubation for several hours, cytoplasmic and nuclear fluorescence can be seen in both cell types (Figure 7B,D). Similar results were observed using NBD-labeled penetratin under the same conditions and in analogous experiments using fluorescent-labeled R_6GC-NH_2 and K_6GC-NH_2 (not shown). These results agree with previous findings indicating that rapid cellular internalization of cell-penetrating peptides such as those examined here occurs via endocytosis (*10*−*14*) and suggest that translocation to other cellular compartments proceeds on a considerably slower time scale (hours rather than minutes).

DISCUSSION

The findings reported here indicate that the previously studied cell-penetrating peptides penetratin and R_6GC-NH_2 (*6*, *9*), as well as the related peptide K_6GC-NH_2, exhibit a substantial ability to translocate into lipid vesicles in a potential-dependent manner and to translocate from an extracytoplasmic compartment to the cytoplasm and nucleus in living mammalian cells. The translocation of these peptides across model (lipid vesicle) membranes is strongly dependent on the bilayer composition as well as the presence of a transbilayer potential.

Previous studies of the abilities of cell-permeant peptides to traverse lipid bilayers have yielded conflicting results. Consistent with our present findings, earlier studies (*22*, *23*) have reported that in the absence of a transbilayer potential, fluorescent-labeled forms of penetratin and the Tat peptide show negligible uptake into vesicles prepared from simple lipid mixtures on a time scale of tens of minutes. By contrast, Thorén et al. (*24*) observed by fluorescence microscopy that over a time course of the order of tens of minutes a Texas Red-labeled penetratin peptide added to the outside of giant unilamellar soybean asolectin vesicles gradually associated not only with the limiting bilayer but also with interior structures that appeared to represent separated internal vesicles. In the present study, however, we observed little uptake of NBD-labeled penetratin into large unilamellar vesicles prepared from the same lipid mixture. It remains unclear whether this apparent discrepancy reflects differences in the nature of the vesicle preparations used, the assay method employed, or some other factor.

The very strong enhancements of vesicle internalization of labeled penetratin, R_6GC-NH_2, or K_6GC-NH_2 that we observe in the presence of a transbilayer potential suggests that a transmembrane potential may play a significant role in the uptake of such peptides into mammalian cells. Maduke and Roise (*34*) have previously demonstrated potential-dependent transbilayer uptake of a positively charged mitochondrial protein presequence, which, however, unlike the peptides examined here exhibits a markedly amphipathic character. Importantly (and strikingly), the observed translocation of penetratin into lipid vesicles can proceed without a major disruption of vesicle integrity, as judged by the very modest effects of penetratin on bilayer leakiness (see, e.g., Figures 4B and 6A,B) and on dissipation of the transbilayer potential (Figure 3). In contrast to some early reports based on microscopic observations of fixed cells, recent findings suggest that cellular uptake of cell-penetrating peptides is energy-dependent and that a large fraction of cell-internalized peptide is localized, at least after short times of incubation with cells, to the endocytic compartment (*10*−*14*). Previous studies have suggested that endocytic compartments exhibit a significant transmembrane potential (lumenal side positive), at least in part through the action of the Na^+,K^+- and possibly the vacuolar-type H^+-ATPase (*47*−*50*). Thus, within at least some subcompartments of the endosomal system, a membrane potential may facilitate translocation of cell-penetrating

peptides from the endosomal lumen to the cytoplasm. It is also of course possible that peptide internalization may occur at least in part through the plasma membrane under the conditions used here and those normally employed to demonstrate biological activities for cell-permeant peptide constructs, in which the peptide is continuously present in the extracellular medium for extended periods.

The observed relationship between the efficiency of potential-dependent penetratin translocation and the bilayer composition suggests that the peptide may traverse lipid bilayers by two different mechanisms. One of these is promoted by the presence of high proportions of lipids that favor the formation of inverted nonbilayer structures (unsaturated phosphatidylethanolamine, phosphatidic acid, cardiolipin, and semilysobis-phosphatidic acid) and is accompanied by significant lipid mixing between vesicles, suggesting that it may proceed through intervesicle contacts and entails at least a limited, local formation of nonlamellar structures. This mechanism of penetratin translocation may resemble that suggested previously by Prochiantz and co-workers (*6*, *51*), in which the formation of inverted nonlamellar structures is hypothesized to play an important role in peptide translocation across bilayers. However, the fact that peptide translocation is accompanied by lipid mixing in the vesicle systems just discussed raises the possibility that interbilayer interactions could play an important role in the mechanism of peptide translocation for these systems.

A second, and apparently distinct, mechanism for translocation of penetratin into lipid vesicles proceeds without significant lipid mixing between vesicles and is favored by lipids whose headgroup cross-sectional areas are relatively large as compared to those of their acyl chains. The detailed nature of this latter pathway of peptide translocation into vesicles remains to be elucidated. One obvious (although at present, entirely speculative) possibility is that penetratin binding to bilayers with such compositions allows the lipids to adopt transient and local structures with net positive surface curvature through which the peptide may translocate across the bilayer (in the presence of a suitable transbilayer potential). This mechanism of transport could resemble in some respects the local electroporation mechanism recently proposed by Binder and Lindblom (*25*). Remarkably, as already noted, neither of the mechanisms of peptide uptake characterized here appears to entail a major loss of vesicle bilayer integrity. In this respect, the translocation of penetratin across bilayers appears to differ significantly from that of more amphiphilic peptides, whose association with lipids typically leads to a major increase in bilayer permeability through the formation of peptide-lined pores or major perturbations of the bilayer organization (*3*−*5*).

The initial rates of potential-dependent translocation of NBD-labeled penetratin, R_6GC-NH_2, or K_6GC-NH_2 that we measure in lipid vesicles under various conditions are fast enough to suggest that a similar mechanism could contribute to the transmembrane permeation of these peptides in living cells, where extended incubation times can be required to observe the accumulation of peptide in nonendocytic compartments. Assessment of this possibility is complicated by our limited knowledge of the precise membrane environments and transmembrane potentials that a cell-penetrating peptide will encounter during the course of its interaction with cells (which may include both association with the plasma membrane and passage through various portions of the endocytic pathway). In this regard, it may be noteworthy that substantial potential-dependent translocation of cationic peptides can be observed into vesicles combining neutral and anionic sphingolipids with unsaturated phosphatidylcholine and cholesterol, which reasonably approximates the lipid composition of the external leaflet of the plasma membrane, as well as into vesicles containing lipids such as lysobis-phosphatidic acid, which are enriched in later compartments of the endosomal/lysosomal system (*52*, *53*). It is also very possible that membrane components other than lipids may enhance the efficiency of the mechanism(s) observed here for potential-dependent translocation of penetratin and other cell-penetrating peptides across lipid bilayers. Nonetheless, the results presented here suggest that interactions with membrane lipids may contribute very importantly to the mechanism of translocation of cell-penetrating peptides across cellular membranes.

ACKNOWLEDGMENT

We thank Dr. Imed Gallouzi for helpful discussions during the course of this work.

REFERENCES

1. Derossi, D., Chassaing, G., and Prochiantz, A. (1998) Trojan peptides: the penetratin system for intracellular delivery, *Trends Cell Biol. 8*, 84−87.
2. Ford, K. G., Souberbielle, B. E., Darling, D., and Farzaneh, F. (2001) Protein transduction: an alternative to genetic intervention? *Gene Ther. 8*, 1−4.
3. Cornut, I., Thiaudière, E., and Dufourcq, J. (1993) The amphipathic helix in cytotoxic peptides, in *The Amphipathic Helix* (Epand, R. M., Ed.) pp 173−219, CRC Press, Boca Raton, FL.
4. Bechinger, B. (1997) Structure and functions of channel-forming peptides: magainins, cecropins, melittin, and alamethicin, *J. Membr. Biol. 156*, 197−211.
5. Nir, S., and Nieva, J. L. (2000) Interactions of peptides with liposomes: pore formation and fusion, *Prog. Lipid Res. 39*, 181−206.
6. Derossi, D., Joliot, A. H., Chassaing, G., and Prochiantz, A. (1994) The third helix of the *Antennapedia* homeodomain translocates through biological membranes, *J. Biol. Chem. 269*, 10444−10450.
7. Derossi, D., Calvet, S., Trembleau, A., Brunissen, A., Chassaing, G., and Prochiantz, A. (1996) Cell internalization of the third helix of the *Antennapedia* homeodomain is receptor-independent, *J. Biol. Chem. 271*, 18188−18193.
8. Vivés, E., Brodin, P., and Lebleu, B. (1997) A truncated HIV-1 Tat protein basic domain rapidly translocates through the plasma membrane and accumulates in the cell nucleus, *J. Biol. Chem. 272*, 16010−16017.
9. Futaki, S., Suzuki, T., Ohashi, W., Yagami, T., Tanaka, S., Ueda, K., and Sugiura, Y. (2001) Arginine-rich peptides. An abundant source of membrane-permeable peptides having potential as carriers for intracellular protein delivery, *J. Biol. Chem. 276*, 5836−5840.
10. Lundberg, M., and Johansson, M. (2002) Positively charged DNA-binding proteins cause apparent cell membrane translocation, *Biochem. Biophys. Res. Commun. 291*, 367−371.
11. Richard, J. P., Melikov, K., Vivés, E., Ramos, C., Verbeure, B., Gait, M. J., Chernomordik, L. V., and Lebleu, B. (2003) Cell-penetrating peptides. A reevaluation of the mechanism of cellular uptake, *J. Biol. Chem. 278*, 585−590.
12. Vivés, E., Richard, J. P., Rispal, C., and Lebleu, B. (2003) TAT peptide internalization: seeking the mechanism of entry, *Curr. Opin. Protein Peptide Sci. 4*, 125−132.
13. Drin, G., Cottin, S., Blanc, E., Rees, A. R., and Temsamani, J. (2003) Studies on the internalization mechanism of cationic cell-penetrating peptides, *J. Biol. Chem. 278*, 31192−31201.

14. Thorén, P. E., Persson, D., Isakson, P., Goksor, M., Onfelt, A., and Nordén, B. (2003) Uptake of analogues of penetratin, Tat-(48−60), and oligoarginine in live cells, *Biochem. Biophys. Res. Commun. 307*, 100−107.
15. Holinger, E. P., Chittenden, T., and Lutz, R. J. (1999) Bak BH3 peptides antagonize Bcl-xL function and induce apoptosis through cytochrome *c*-independent activation of caspases, *J. Biol. Chem. 274*, 13298−13304.
16. Dui, J., Feng, L., Yang, F., and Lu, B. (2000) Activity- and Ca^{2+}-dependent modulation of surface expression of brain-derived neurotrophic factor receptors in hippocampal neurons, *J. Cell Biol. 150*, 1423−1434.
17. Gallouzi, I.-E., and Steitz, J. A. (2001) Delineation of mRNA export pathways by the use of cell-permeable peptides, *Science 294*, 1895−1901.
18. Stolzenberger, S., Haake, M., and Duschl, A. (2001) Specific inhibition of interleukin-4-dependent Stat6 activation by an intracellularly delivered peptide, *Eur. J. Biochem. 268*, 4809−4814.
19. Joliot, A., Pernelle, C., Deagostini-Bazin, H., and Prochiantz, A. (1991) Antennapedia homeobox peptide regulates neural morphogenesis, *Proc. Natl. Acad. Sci. U.S.A. 88*, 1864−1868.
20. Drin, G., Mazel, M., Clair, P., Mathieu, D., Kaczorek, M., and Temsamani, J. (2001) Physicochemical requirements for cellular uptake of pAntp peptide. Role of lipid-binding affinity, *Eur. J. Biochem. 268*, 1304−1314.
21. Berlose, J. P., Convert, O., Derossi, D., Brunissen, A., and Chassaing, G. (1996) Conformational and associative behaviours of the third helix of *Antennapedia* homeodomain in membrane-mimetic environments, *Eur. J. Biochem. 242*, 372−386.
22. Drin, G., Demene, H., Temsamani, J., and Brasseur, R. (2001) Translocation of the pAntp peptide and its amphipathic analogue AP-2AL, *Biochemistry 40*, 1824−1834.
23. Kramer, S. D., and Wunderli-Allenspach, H. (2003) No entry for TAT(44−57) into liposomes and intact MDCK cells: novel approach to study membrane permeation of cell-penetrating peptides, *Biochim. Biophys. Acta 1609*, 161−169.
24. Thorén, P. E., Persson, D., Karlsson, M., and Nordén, B. (2000) The antennapedia peptide penetratin translocates across lipid bilayers—the first direct observation, *FEBS Lett. 482*, 265−268.
25. Binder, H., and Lindblom, G. (2003) Charge-dependent translocation of the Trojan peptide penetratin across lipid membranes, *Biophys. J. 85*, 982−995.
26. Lowry, R. R., and Tinsley, I. J. (1974) A simple, sensitive method for lipid phosphorus, *Lipids 9*, 491−492.
27. Kagawa, Y., Kandrach, A., and Racker, E. (1973) Partial reconstitution of the enzymes catalyzing oxidative phosphorylation. XXVI. Specificity of phospholipids required for energy transfer reactions, *J. Biol. Chem. 248*, 676−684.
28. Monti, J. A., Christian, S. T., and Shaw, W. A. (1978) Synthesis and properties of a highly fluorescent derivative of phosphatidylethanolamine, *J. Lipid Res. 19*, 22−28.
29. Struck, D. K., Hoekstra, D., and Pagano, R. E. (1981) Use of resonance energy transfer to monitor membrane fusion, *Biochemistry 20*, 4093−4099.
30. Schroeder, H., Leventis, R., Shahinian, S., Walton, P. A., and Silvius, J. R. (1996) Lipid-modified, cysteinyl-containing peptides of diverse structures are efficiently S-acylated at the plasma membrane of mammalian cells, *J. Cell Biol. 134*, 647−660.
31. Quesnel, S., and Silvius, J. R. (1994) Cysteine-containing peptide sequences exhibit facile uncatalyzed transacylation and acyl-CoA-dependent acylation at the lipid bilayer interface, *Biochemistry 33*, 13340−13348.
32. MacDonald, R. C., MacDonald, R. I., Menco, B. P., Takeshita, K., Subbarao N. K., and Hu, L. R. (1991) Small-volume extrusion apparatus for preparation of large, unilamellar vesicles, *Biochim. Biophys. Acta 1061*, 297−303.
33. Skerjanc, I. S., Shore, G. C., and Silvius, J. R. (1987) The interaction of a synthetic mitochondrial signal peptide with lipid membranes is independent of transbilayer potential, *EMBO J. 6*, 3117−3123.
34. Maduke, M., and Roise, D. (1993) Import of a mitochondrial presequence into protein-free phospholipid vesicles, *Science 260*, 364−367.
35. Allen, T. M., and Cleland, L. G. (1980) Serum-induced leakage of liposome contents, *Biochim. Biophys. Acta 597*, 418−426.
36. McIntyre, J. C., and Sleight, R. G. (1991) Fluorescence assay for phospholipid membrane asymmetry, *Biochemistry 30*, 11819−11827.
37. Leventis, R., and Silvius, J. R. (1998) Lipid-binding characteristics of the polybasic carboxy-terminal sequence of K-ras4B, *Biochemistry 37*, 7640−7648.
38. Persson, D., Thorén, P. E., Herner, M., Lincoln, P., and Nordén, B. (2003) Application of a novel analysis to measure the binding of the membrane-translocating peptide penetratin to negatively charged liposomes, *Biochemistry 42*, 421−429.
39. Montich, G., Scarlata, S., McLaughlin, S., Lehrmann, R., and Seelig, J. (1993) Thermodynamic characterization of the association of small basic peptides with membranes containing acidic lipids, *Biochim. Biophys. Acta 1146*, 17−24.
40. Mayer, L. D., Bally, M. B., Hope, M., and Cullis, P. R. (1985) Uptake of dibucaine into large unilamellar vesicles in response to a membrane potential, *J. Biol. Chem. 260*, 802−808.
41. de Kroon, A. I., Vogt, B., van't Hof, R., de Kruijff, B., and de Gier, J. (1991) Ion gradient-induced membrane translocation of model peptides, *Biophys. J. 60*, 525−537.
42. Sims, P. J., Waggoner, A. S., Wang, C.-H., and Hoffman, J. F. (1974) Studies on the mechanism by which cyanine dyes measure membrane potential in red-blood cells and phosphatidylcholine vesicles, *Biochemistry 13*, 3315−3330.
43. Gruner, S. M., Cullis, P. R., Hope, M. J., and Tilcock, C. P. (1985) Lipid polymorphism: the molecular basis of nonbilayer phases, *Annu. Rev. Biophys. Biophys. Chem. 14*, 211−238.
44. Cullis, P. R., Hope, M. J., and Tilcock, C. P. (1986) Lipid polymorphism and the roles of lipids in membranes, *Chem. Phys. Lipids 40*, 127−144.
45. Cullis, P. R., de Kruijff, B., Verkleij, A. J., and Hope, M. J. (1986) Lipid polymorphism and membrane fusion, *Biochem. Soc. Trans. 14*, 242−245.
46. Mosior, M., and McLaughlin, S. (1992) Electrostatics and reduction of dimensionality produce apparent cooperativity when basic peptides bind to acidic lipids in membranes, *Biochim. Biophys. Acta 1105*, 185−187.
47. Van Dyke, R. W. (1988) Proton pump-generated electrochemical gradients in rat liver multivesicular bodies. Quantitation and effects of chloride, *J. Biol. Chem. 263*, 2603−2611.
48. Fuchs, R., Schmid, S., and Mellman, I. (1989) A possible role for the Na^+,K^+-ATPase in regulating ATP-dependent endosomal acidification, *Proc. Natl. Acad. Sci. U.S.A.* 86, 539−543.
49. Van Dyke, R. W., and Belcher, J. D. (1994) Acidification of three types of liver endocytic vesicles: similarities and differences, *Am. J. Physiol. 266*, C81−C94.
50. Rybak, S. L., Lanni, F., and Murphy, R. F. (1997) Theoretical considerations on the role of membrane potential in the regulation of endosomal pH, *Biophys. J. 73*, 674−687.
51. Prochiantz, A. (1996) Getting hydrophilic compounds into cells: lessons from homeopeptides, *Curr. Opin. Neurobiol. 6*, 629−634.
52. Brotherus, J., and Renkonen, O. (1977) Subcellular distributions of lipids in cultured BHK cells: evidence for the enrichment of lysobisphosphatidic acid and neutral lipids in lysosomes, *J. Lipid Res. 18*, 191−202.
53. Kobayashi, T., Gu, F., and Gruenberg, J. (1998) Lipids, lipid domains, and lipid−protein interactions in endocytic membrane traffic, *Semin. Cell Dev. Biol. 9*, 517−526.

BI035293Y